Horizontal Grids and Map Projections

Learning Outcomes

Following this lecture, students will be able to:

- Understand the differences between structured and unstructured model grids.
- Describe what is meant by grid staggering and why it is used.
- Describe the key characteristics that must be preserved when projecting the spherical Earth onto a flat three-dimensional model grid and identify the map projection with the characteristics that satisfy the most important of these requirements.
- Quantify and conceptually describe what is meant by a map-scale factor.
- Conceptually describe differences between methods for variable grid resolution.

Structured and Unstructured Grids

Most modern numerical weather prediction models, particularly those used to obtain forecasts over limited-area domains, use grid-based methods to discretize the atmosphere into coherent points or blocks over which the primitive equations are solved. Such a grid may be structured or unstructured in nature:

- A **structured grid** is one in which the grid is regular; e.g., rectangles with sides of uniform length over the entire domain. Such sides may be defined by physical distance (e.g., each grid box has sides of length 4 km) or by latitude and longitude (e.g., each grid box has sides of length 0.04° latitude and longitude). An example of a structured grid is given in Fig. 1 (left).
- An **unstructured grid** is one in which the grid is irregular; e.g., triangles or hexagons with sides of variable length across the domain. Unstructured grids require that information about the model grid's construction be retained in memory throughout its execution. An example of an unstructured grid is given in Fig. 1 (right).

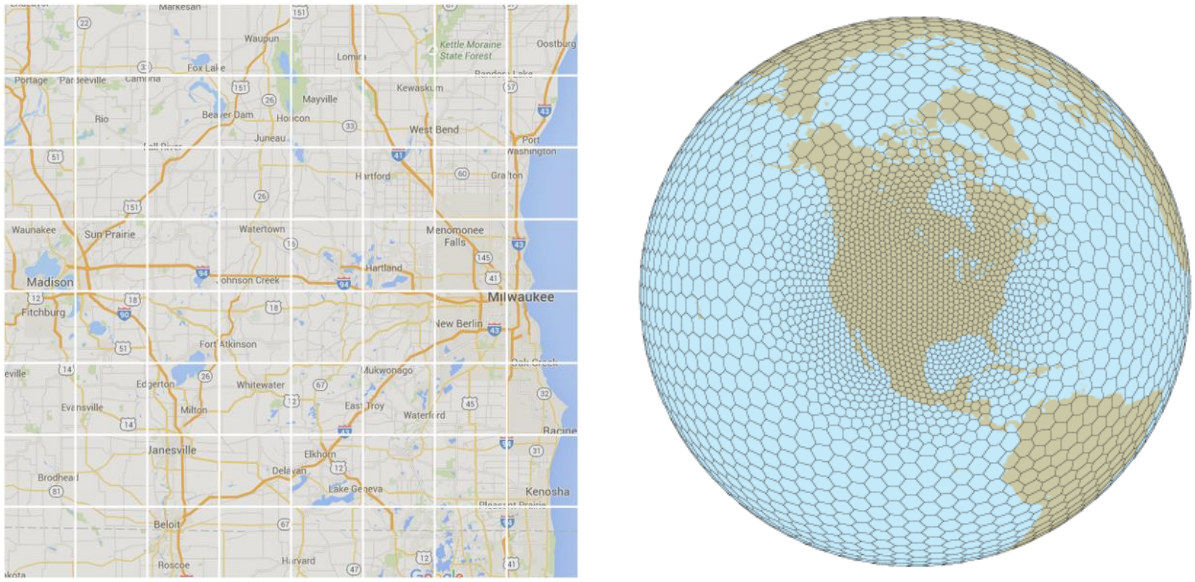

Figure 1. (left) An example of a structured grid, with sides of uniform distance, applied to southeastern Wisconsin. (right) An example of an unstructured grid, constructed of hexagons with sides of variable length, across the Western Hemisphere. Image at right obtained from https://mpas-dev.github.io/atmosphere/atmosphere.html.

Grid Staggering

Model variables may be defined on what are known as **staggered grids**, wherein mass-related fields such as pressure and temperature are defined on one set of grid points while velocity fields are defined on another set of grid points. Both horizontal and vertical grids may be staggered.

Staggered grids allow for certain partial derivatives, such as the advection of a mass-related field, to be evaluated over a smaller grid interval. Because the grid interval for these partial derivatives is decreased, however, models using staggered grids must use a smaller timestep to maintain computational stability. Note also that wave dispersion on certain staggered grids is more realistic than on an unstaggered grid.

There are five *horizontal* model grids, referred to as the Arakawa "A" through "E" grids, as depicted in Fig. 2 (Arakawa and Lamb 1977, *Methods of Computational Physics*). The Arakawa "A" grid is unstaggered; all model variables are defined at the same points, whether at the grid corners (as pictured) or at the grid center. The other four grids are staggered.

Of the four unstaggered grids, the "B" and "E" grids are similar to each other, whereas the "C" and "D" grids are similar to each other. For the "B" grid, mass-related variables are defined at the grid corners and velocity variables are defined at the grid center, or vice versa. The North American Mesoscale, or NAM, model is an example of a model that uses a "B" grid. The Arakawa "E" grid is akin to the "B" grid, except rotated 45°. On "E" grids, adjacent points for a

given variable are along diagonals rather than a purely horizontal or vertical path. The Hurricane WRF, or HWRF, model is an example of a model that uses an "E" grid.

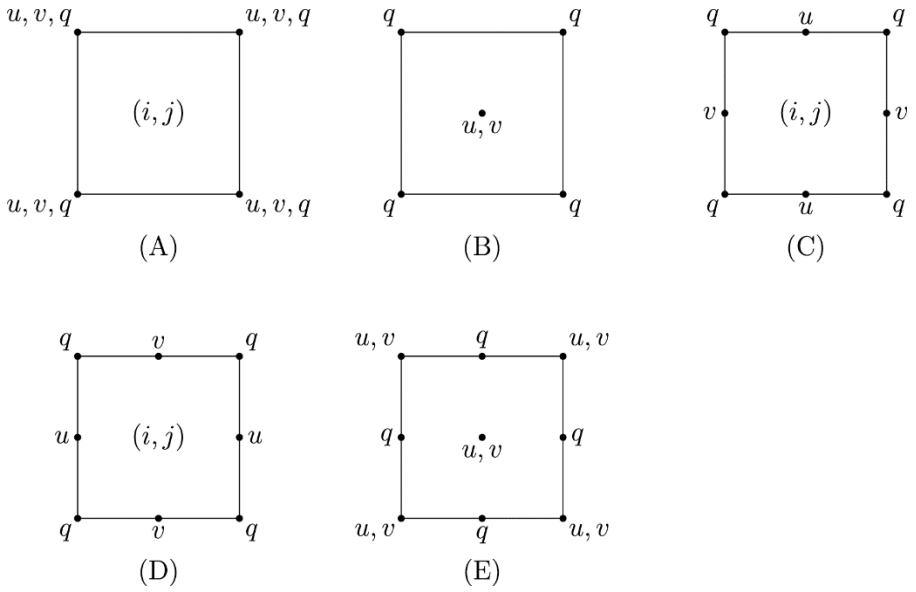

Figure 2. Spatial discretization of model variables on the Arakawa "A" through "E" grids. In each panel, *u* and *v* are the horizontal wind components and *q* is a generic mass-related variable. Please refer to the text for further details regarding each grid. Figure obtained from Wikimedia Commons via author JuliusSimplus and used under a CC BY-SA 3.0 license.

Unlike the "B" and "E grids, velocity variables *u* and *v* on the "C" grid are staggered with respect to each other. This staggered grid most commonly takes the form given by Fig. 3 (left), with mass-related variables defined at the grid center and *u* and *v* defined normal to grid cell edges. This configuration allows for the horizontal divergence – which appears in many of the primitive equations – to be defined coincident with the mass-related variables (which makes physical sense since this is the *mass* divergence). Many modern grid-point models, including the WRF-ARW and MPAS models, use Arakawa "C" grids.

The "D" grid is a 90° rotation of a "C" grid. Rather than *u* and *v* defined normal to grid cell edges, *u* and *v* on the "D" grid are defined parallel to grid cell edges. This configuration allows for vorticity rather than divergence to be defined coincident with the mass-related variables. This does not provide the advantages that horizontal divergence does with the "C" grid, however. Furthermore, studies have shown that the "D" grid does not handle wave dispersion as well as the "B," "C," and "E" grids and, consequently, it is not commonly used in modern models.

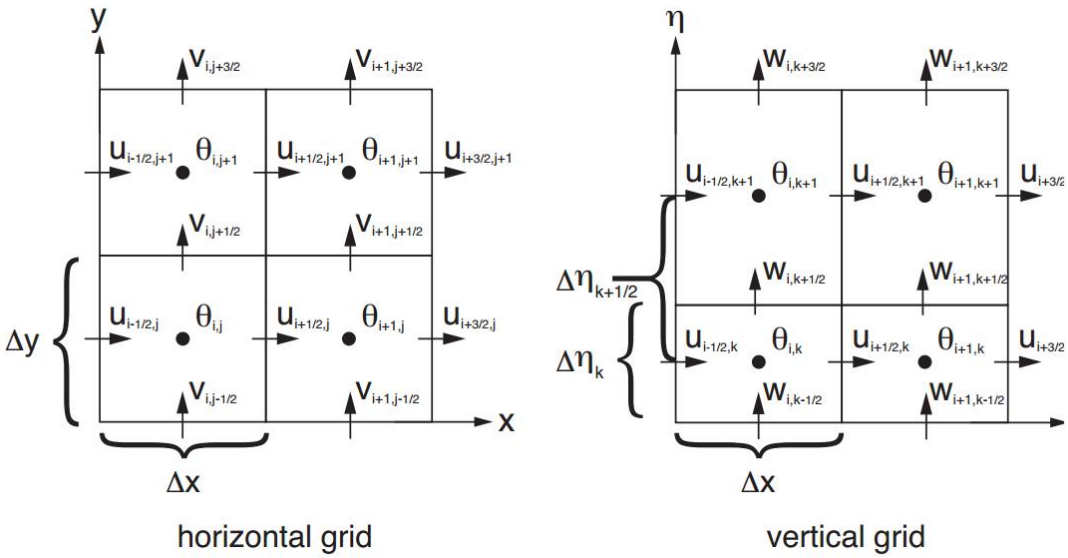

Figure 3. (left) Arakawa "C" grid as utilized within the WRF-ARW model, with horizontal velocities (u, v) defined normal to grid cell edges and mass-related fields (θ, μ, q_m, p, α) defined at grid centers. (right) Vertical staggered grid as utilized within the WRF-ARW model, with vertical velocity ω and geopotential ϕ defined at the top and bottom of a vertical grid cell. Note that ω and ϕ are defined atop mass-related fields. Reproduced from https://opensky.ucar.edu/islandora/object/opensky:2898, their Fig. 3.2.

The most common type of staggered *vertical* grid is one where vertical velocity and geopotential are defined at the top and bottom of a vertical grid cell and all other model variables are defined at the center of a vertical grid cell. A graphical example is given in Fig. 3 (right).

Why would vertical velocity and geopotential be defined on the grid cell edges? If we take the total derivative of the geopotential ($\Phi = gz$), a diagnostic relationship between the geopotential and the vertical velocity ($w = Dz/Dt$) results. Further, defining vertical velocity at the top and bottom of vertical grid cells allows us to specify no vertical velocity through the lower model boundary as a lower model boundary condition, a physically rooted specification.

How is grid staggering manifest in practice? Consider a simplified u-momentum equation:

$$\frac{\partial u}{\partial t} = -u\frac{\partial u}{\partial x} - v\frac{\partial u}{\partial y} - w\frac{\partial u}{\partial z} + fv - \frac{1}{\rho}\frac{\partial p}{\partial x}$$

Let us assume that model variables are defined on an Arakawa "C" grid. As illustrated by Fig. 3, the only model variable defined at the grid points where u is defined is u itself. The Arakawa "C" grid staggering of the mass-related variables allows the horizontal pressure gradient term to also be evaluated at the grid points where u is defined.

However, interpolating the other model variables to the *u* grid points is necessary to solve the equation above. For density ρ, a mass-related field, this is straightforward: compute the average of the densities defined at the adjacent mass-related grid points in the *x*-direction (e.g., at points *x+1/2* and *x-1/2*). For *v* and *w*, this is more complicated due to how they are staggered with respect to *u*. First, compute the average *v* or *w* at the mass-related grid points in the *x*-direction adjacent to the *u* grid point. Next, compute the average *v* or *w* between these adjacent mass-related grid points in the *x*-direction. The interpolation between grids required with staggered grids introduces some error into the model formulation, but the benefits of staggered grids (especially the Arakawa "C" grid) typically outweigh this added interpolation error.

Map Projections

Limited-area grid-point models use *map projections*, which are mathematical relationships that transform a portion of the spherical Earth to a horizontal grid. There are several desirable traits for a chosen map projection:

- **Preserves angles**. Angles on the grid should be equivalent to those on the Earth.
- **Preserves areas**. Areas on the grid should be equivalent to those on the Earth. This implies that *distances* on the grid should be equivalent to those on the Earth.
- **Preserves shapes**. Shapes on the grid should be equivalent to those on the Earth.
- **Correct directions**. Directions on the grid should be equivalent to those on the Earth.
- The shortest distance between two lines should be a great circle, as it is on the Earth.

No individual map projection can satisfy all of these traits. In the atmospheric sciences, the most desirable of these traits is that **angles be preserved**. This allows for an accurate, straightforward representation of the horizontal wind components (*u*, *v*) and meteorological fields derived from them (e.g., vorticity and divergence) on the model grid.

A **conformal** map projection is one in which angles are inherently preserved. The defining characteristic of a conformal map is that latitude and longitude lines are *locally perpendicular* everywhere on the map. However, conformal maps do not preserve shapes, distances, or areas. Near what are known as the *standard parallels* of the projection, where the cone, cylinder, or planar surface onto which the Earth is projected intersect the Earth, shape, distance, and area distortion are small. Away from the standard parallels, however, these distortions can be large. The choice of which map projection to use for a given limited-area model domain is made with respect to the range of latitudes over which its distortion is relatively small.

The three most commonly used conformal map projections in numerical weather prediction and the atmospheric sciences in general are the **Lambert conic**, **Mercator**, and **polar stereographic** map projections. Schematics of each are presented in Fig. 4 below.

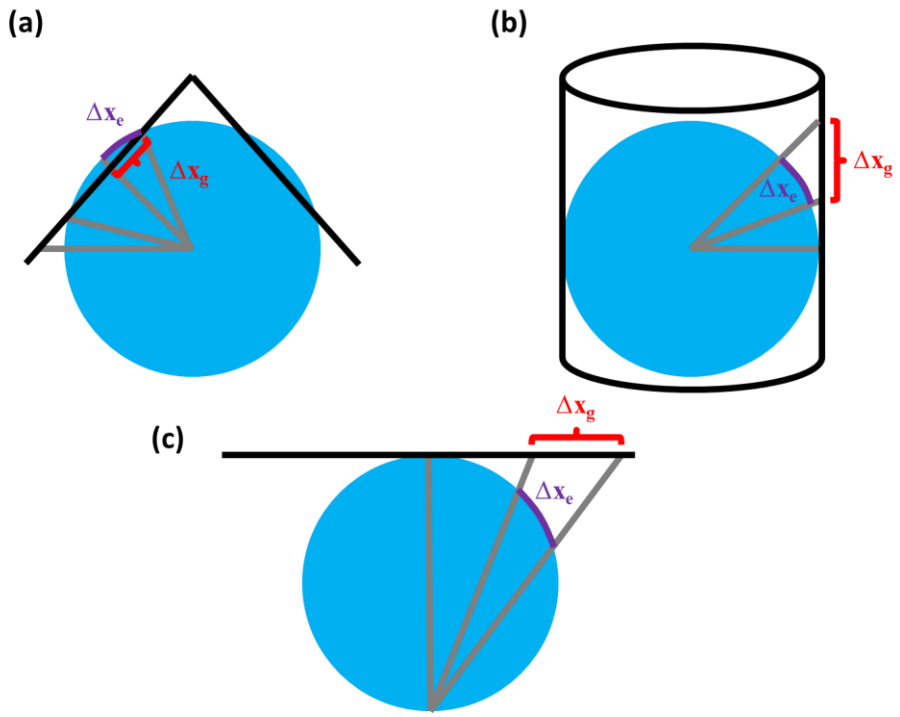

Figure 4. Graphical schematics of the (a) Lambert conic, (b) Mercator, and (c) polar stereographic conformal map projections. Please refer to the text for additional details.

The Lambert conic projection is obtained by fitting a cone with its tip located above the North or South Pole either tangent or secant to the Earth. The Lambert conic projection is constructed by projecting outward from the center of the Earth to the fitted cone. The schematic in Fig. 4 is an example of the more commonly used secant fit, with the cone's surface intersecting the Earth at two secant points. These points define the projection's standard parallels and are typically ~30°N and ~60°N. Map distortion for this projection is smallest near the secant or tangent points.

The Mercator projection is obtained by fitting a cylinder with its vertical axis located along the Earth's poles tangent or secant to the Earth. The Mercator projection is constructed by projecting outward from the center of the Earth to the fitted cylinder. The schematic in Fig. 4 is an example of the more commonly used tangent fit, where the cylinder's surface intersects the Earth at one point (typically at the Equator, defining a single standard parallel for this projection). Map distortion for this projection is smallest in the tropics.

The polar stereographic projection is obtained by placing a flat planar surface parallel to the Earth's equator either tangent or secant to the Earth near the North or South Pole. The schematic in Fig. 4 is an example of a tangent fit, where the surface intersects the Earth at the North Pole. Both tangent and secant fits to the Earth are common with polar stereographic projections, and the definition of the standard parallel(s) for each are similar to those for the Lambert conic and Mercator projections described above. Polar stereographic projections are constructed by projecting outward from the opposite pole to the planar surface. Map distortion for this projection is smallest near the poles.

The distance distortion can be quantified by the **map-scale factor**, or *m*. For each projection, the map-scale factor is generally defined as the *distance between points on the model grid* divided by the *distance between points on the Earth*, i.e.,

$$m = \frac{\Delta x_g}{\Delta x_e}$$

where Δx_g (distance on the model grid) and Δx_e (corresponding distance on the Earth) are defined graphically in Fig. 4. Even though *m* is defined in terms of Δx, note that *m* is constant between the zonal and meridional directions for conformal map projections.

At the standard parallels, $m = 1$. For secant projections, $m < 1$ ($\Delta x_g < \Delta x_e$) between the standard parallels and $m > 1$ ($\Delta x_g < \Delta x_e$) outside of the standard parallels. For tangent projections, $m > 1$ away from the standard parallel.

Using spherical geometry, precise relationships for *m* for each projection may be obtained. These are provided below, assuming a tangent fit to the cylinder for the Mercator projection and secant fits for the Lambert conic and polar stereographic projections.

$$m = \frac{\sin\phi_{ref}}{\sin\phi}\left(\frac{\tan\left(\frac{\phi}{2}\right)}{\tan\left(\frac{\phi_{ref}}{2}\right)}\right)^n, \text{ where } n = \frac{\ln\left(\frac{\sin\phi_{ref1}}{\sin\phi_{ref2}}\right)}{\ln\left(\frac{\tan\left(\frac{\phi_{ref1}}{2}\right)}{\tan\left(\frac{\phi_{ref2}}{2}\right)}\right)} \qquad \text{(Lambert conic)}$$

$$m = \sec\phi \qquad \text{(Mercator)}$$

$$m = \frac{1+\sin\phi_{ref}}{1+\sin\phi} \qquad \text{(Polar stereographic)}$$

In the above, ϕ is latitude and subscripts of *ref* refer to the standard parallels. Note that the map-scale factor for these and all conformal projections, is equal in the *x* and *y* directions.

Graphs of the map-scale factor for each projection as a function of latitude are presented in Fig. 5. We desire that $m \approx 1$ over the range of latitudes considered within our simulation domain. Thus, the Mercator projection is ideally suited for the tropics, the Lambert conic projection is ideally suited for the midlatitudes, and the polar stereographic projection is ideally suited for higher latitudes. Secant forms of each projection typically are applicable over a wider range of latitudes than their corresponding tangent forms.

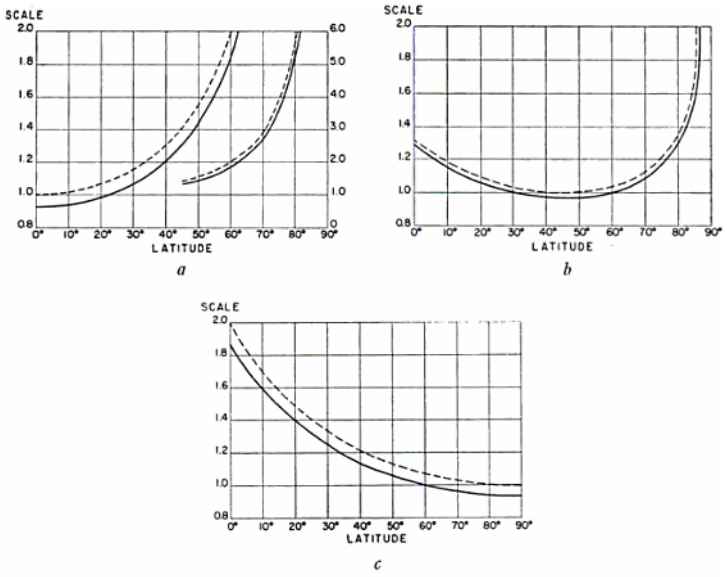

Figure 5. Map-scale factors as a function of latitude for the (a) Mercator, (b) Lambert conic, and (c) polar stereographic map projections. In each panel, solid (dashed) lines refer to the map-scale factor for secant (tangent) forms of each projection. The standard parallels for the secant projections are (a) 20°S and 20°N, (b) 30°N and 60°N, and (c) 60°N. The standard parallels for the tangent projections are (a) 0°, (b), 45°N, and (c) 90°N. For the Mercator projection, the second set of curves scales with the *y*-axis on the right side of the panel. Figure reproduced from Saucier (1955, *Principles of Meteorological Analysis*), their Fig. 2.113.

Latitude-Longitude Grids

It is also possible to use a non-conformal latitude-longitude, or *equirectangular cylindrical*, map projection. Like a Mercator projection, the latitude-longitude map projection is based on representing the spherical Earth on a cylinder's surface. However, whereas the Mercator projection is obtained by literally projecting the Earth onto the cylinder's surface, the latitude-longitude map projection is obtained simply by unfurling the Earth's surface onto the surface of a cylinder that is tangent to the Earth at the Equator.

Unlike conformal map projections, which are associated with equal horizontal grid spacing in terms of *distance* (e.g., constant Δx_g), latitude-longitude grids are associated are associated with equal horizontal grid spacing in terms of *latitude and longitude*. Models that utilize latitude-longitude map projections will often pose the primitive equations in spherical coordinates, where the horizontal coordinates are latitude and longitude rather than the Cartesian coordinates *x* and *y*. While it is possible for a limited-area model grid to be constructed from the latitude-longitude map projection, this map projection is more commonly associated with global model grids.

Latitude-longitude map projections are not conformal; as a consequence, the map-scale factor for latitude-longitude map projections is different in the *x* and *y* directions. Because the distance between latitudes is constant with latitude (1° = 111,177 m), there is no map distortion in the meridional (north-south) direction, so that the map-scale factor m_y is 1. The map distortion in the zonal (east-west) direction is a function of latitude, where:

$$m_x = \sec \phi$$

This value is 1 at the Equator and increases slowly through the tropics, more rapidly through the midlatitudes, and exponentially grows approaching the poles. Thus, the least distance distortion in the zonal direction with the latitude-longitude projection is found in the tropics.

Because latitude-longitude grids are based on discrete increments of latitude and longitude, there is a singularity at the North and South Poles where all meridians (or lines of constant longitude) converge. As one approaches the poles, the physical distance between individual grid points along parallels approaches zero. This necessitates a small time step to maintain computational stability. The added computational expense that results generally far exceeds the added benefit from implicitly finer model resolution.

Models using latitude-longitude grids can handle this in one of two ways. One method, as is used by the WRF-ARW model, involves applying a Fourier filter to the model fields near the poles to truncate high wavenumber (e.g., small-scale) variability. This permits the use of a longer model time step despite a comparatively large number of grid points over a small area, though it still necessitates solving the primitive equations on the relatively dense grid near the poles. This Fourier filter in the WRF-ARW model takes the form given in Section 4.1 of Skamarock et al. (2021):

$$\hat{\varphi}_{filtered}(k) = a(k)\hat{\varphi}(k)$$

Here, *k* is a dimensionless wavenumber, *a*(*k*) is the filter function, $\hat{\varphi}(k)$ are the Fourier coefficients for a generic variable φ before filtering, and $\hat{\varphi}_{filtered}(k)$ are the Fourier coefficients for a generic variable φ after filtering. The $\hat{\varphi}(k)$ are obtained by applying a one-dimensional Fourier transform to φ on the constant latitude-longitude grid; the filtered variable φ is then

obtained by applying a one-dimensional inverse transform given filtered Fourier coefficients $\hat{\varphi}_{filtered}(k)$.

The filter function $a(k)$ takes the form:

$$a(k) = \min\left[1, \max\left(0, \left(\frac{\cos\phi}{\cos\phi_0}\right)^2 \left(\frac{1}{\sin^2(\pi k / n)}\right)\right)\right]$$

Here, ϕ is latitude, ϕ_0 is the latitude above which the polar filter is applied (with no filtering at lower latitudes), and n is the number of zonal grid points along a parallel. n is determined from the chosen horizontal grid spacing. At higher latitudes, cos ϕ approaches zero, such that the value of $a(k)$ approaches zero approaching the poles. Thus, greater filtering is applied at higher latitudes. Generally speaking, the $\sin^2$ function permits the retention of variability with wavelengths of approximately $2\Delta x$ and larger.

Another method is to use a *reduced latitude-longitude grid*. In this method, the spacing between latitude and longitude points is not constant across the model grid; instead, the spacing between longitude points gets larger approaching the poles. A hypothetical example of this is a latitude-longitude grid with grid spacing of 0.2° latitude at all latitudes and grid spacing of 0.2° longitude between the Equator and 60°N/S that grows to 2° at the poles.

Numerical Considerations of Conformal and Latitude-Longitude Map Projections

Fundamentally, the primitive equations apply to the Earth; in other words, ∂x and ∂y are finite displacements in the x and y directions, respectively, *on the Earth*. The horizontal velocities u and v are related to position displacements *on the Earth*. However, with a numerical model, ∂x and ∂y are finite displacements in the x- and y-directions, respectively, *on the model grid*.

For conformal map projections, the physical distance Δx_e between grid points varies across the grid as a function of the map-scale factor m, where $\Delta x_e = \Delta x_g / m$. For latitude-longitude map projections, the physical distance Δx_e between meridional grid points does not vary across the grid; however, the physical distance Δx_e between zonal grid points does vary across the grid as a function of the map-scale factor m_x.

Consequently, the model's version of the primitive equations must account for the departure of the horizontal grid spacing Δx_g from Δx_e. This is accomplished by redefining the model's kinematic variables with respect to the map-scale factor and recasting the spatial partial derivatives in terms of the map-scale factor and distance on the model grid. The redefined versions of the primitive equations in the WRF-ARW model are given by equations (2.15), (2.16), and (2.18) through (2.24) of Skamarock et al. (2021).

There are two important considerations to keep in mind when considering these equations:

- When considering numerical stability for models that use a map projection, the Δx in the Courant number and CFL criterion refers to Δx_e. Because Δx_e varies across the grid, this means that the CFL criterion also can vary across the grid. Furthermore, because $m \geq 1$ except between the standard parallels of a secant map projection, this means that $\Delta x_e \leq \Delta x_g$. This necessitates using a smaller time step Δt to maintain numerical stability than would be necessary if no map projection were used.

- Latitudinal variability in the map-scale factor near the secant or tangent points of conformal map projections and near the Equator for latitude-longitude map projections is relatively small. Conversely, it is large away from these latitudes, as can be inferred from Fig. 5. This latitudinal variability introduces a large non-physical correction to the primitive equations.

As a result of these and other considerations, the choice of map projection for a given simulation domain is motivated by a desire to *minimize distance distortion* (i.e., departures of Δx_e from Δx_g) and to *minimize latitudinal variability in the map-scale factor*. A review of Fig. 5 suggests that both may be accomplished by choosing the map projection based upon where the map-scale factor is closest to 1 over the widest range of latitudes covered by the simulation domain. In other words, apply the latitude-longitude map projection globally or in the tropics, the Mercator map projection in the tropics, the Lambert conic map projection in the midlatitudes, and the polar stereographic map projection at higher latitudes.

The exact forms of the curvature and Coriolis terms in the *u*-, *v*-, and *w*-momentum equations depend on the chosen map projection. For the WRF-ARW model, these are given by equations (2.25) – (2.27) of Skamarock et al. (2021).

Spherical Geodesic Grids

A *geodesic* is the shortest possible line between two points on a sphere or other curved surface. On a sphere, we know geodesics as *great circles*. The roughly spherical Earth can be discretized into a *spherical geodesic grid* by dividing it into a collection of equilateral triangles whose sides are geodesics. Because of using geodesics to define the model grid, spherical geodesic grids are associated with minimal distance distortion between the Earth and model grid. The Model for Prediction Across Scales (MPAS) model is an example of a modern model that uses a spherical geodesic grid.

The process of discretizing the Earth on a spherical geodesic grid is illustrated in Fig. 6. We begin by fitting an icosahedron – a three-dimensional geometric solid with twenty triangular faces, twelve vertices, and thirty sides – to the spherical Earth. The twelve vertices are positioned such that they touch the spherical surface (Fig. 6a).

Next, this grid may be refined by subdividing the twenty triangular faces. For example, bisecting (or splitting in half) each side of a spherical triangle and connecting the subdivision points (Fig. 6b) results in four new flat triangular faces for each original triangular face. The new vertices that result from this subdivision – the bisection points – are then positioned such that they also touch the spherical surface (Fig. 6c). Replacing the lines between subdivision points with geodesics transforms the flat triangular faces into spherical grid triangles (Fig. 6d). Repeating this refinement process can further refine the grid until the desired horizontal grid spacing is achieved. The resulting horizontal grid spacing is the geodesic distance between the centers of adjacent grid cells.

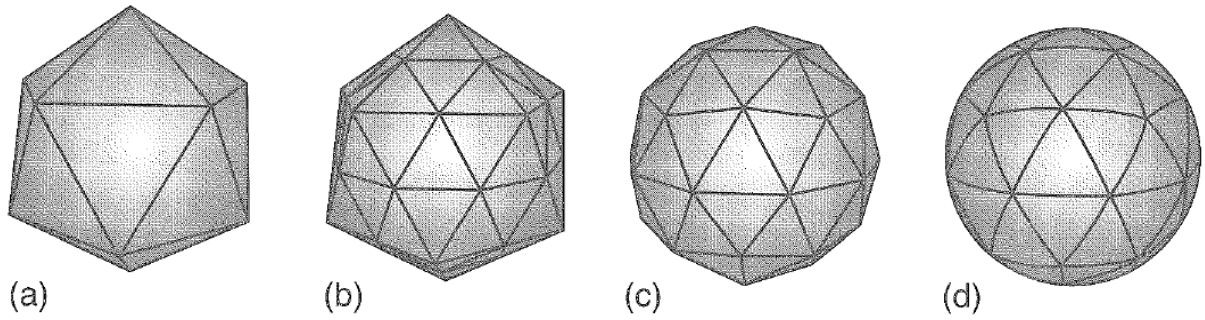

Figure 6. Schematic depicting the process of constructing a spherical geodesic grid by fitting an icosahedron to the spherical Earth and subdividing it with spherical triangular faces. Please refer to the text for further details. Reproduced from Warner (2011), their Fig. 3.10.

Looking closely at Fig. 6d, the northwestern-most visible vertex is the intersection of five triangles, representing the center point of a spherical pentagon. However, the next vertex to the east, in the north-center portion of the grid, is the intersection of six triangles, representing the center point of a spherical hexagon. Spherical geodesic grids thus contain a combination of spherical pentagons and hexagons, and the distances along the sides of these features differ slightly from each other. This results in a small degree of distance distortion.

The spherical geodesic refinement need not be done uniformly across the sphere. If refined in a non-uniform fashion, the refinement process allows for variable resolution across the domain.

Spherical geodesic grids are *unstructured* grids. Thus, information regarding how the model grid is arranged – e.g., the locations of each grid center – must be carried with the model during its integration. For structured grids such as those defined based upon conformal and latitude-longitude map projections, this is not true; adjacent points are simply one point away in the *x*/longitude or *y*/latitude dimension.

Spherical geodesic grids also need not necessarily result from a triangular refinement. For instance, a hexagonal refinement can also be used. This is the approach taken by the MPAS model, as illustrated in Fig. 1 (right). The hexagonal refinement is obtained from a triangular refinement, such as illustrated in Fig. 7, as follows. Identify the bisection point of each spherical triangle's side. Draw a geodesic line through this point perpendicular to each spherical triangle's side. Terminate these geodesic lines where they intersect with each other. The resultant spherical polygons are hexagons whose centers are triangle vertices. The hexagons encompass the portions of each triangle that lies closest to the hexagon's centers.

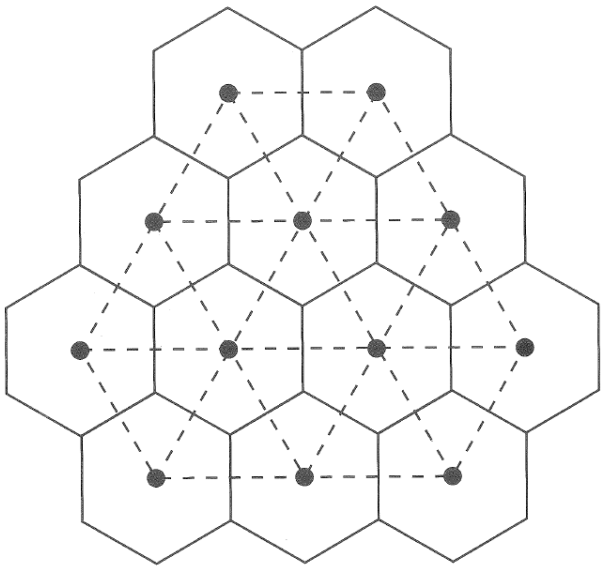

Figure 7. The relationship between triangular and hexagonal refinements of a spherical geodesic grid. Reproduced from Warner (2011), their Fig. 3.12.

Spherical geodesic grids are often used in *finite-volume* models, although not all finite-volume models use spherical geodesic grids. For instance, the Finite Volume 3 model core used by the GFS model is an example of a finite-volume model that does not use a spherical geodesic grid. As compared to traditional grid-point models that consider model variables only at grid points, which are assumed to be representative of the entire grid cell, finite-volume models consider the grid-cell-averaged values of model variables.

Methods for Variable Horizontal Grid Resolution

Independent of the grid structure and map projection used, it is possible to construct a model configuration with variable horizontal grid resolution. The primary benefit to doing so is to allow

for finer discretization over an area or for a feature of interest while minimizing the computational expense that would result from finer discretization over the entire domain. The precise means by which variable grid resolution is achieved depends on whether an unstructured or structured grid is used, and there exist multiple options for doing so in the latter case.

Unstructured grids generally permit variable grid resolution simply by adding or removing grid elements within a region of interest. The example provided in Fig. 1 (right) is an example of a variable resolution unstructured grid, with horizontal grid spacing of ~60 km over much of the globe gradually reducing to ~15 km over North America. Other grid discretizations are possible.

It is not as straightforward to use variable grid resolution with structured grids. There exist two primary approaches to doing so: nested domains and grid stretching. *Nested domains* reflect the case where the model is integrated over multiple, often telescoping domains. Examples of nested domains are given in Figs. 8 and 9. A nested grid is often referred to as a child domain, whereas the grid that surrounds the nested grid is often referred to as a parent domain. In the example below, the outermost grid is the parent of the intermediate grid, which is the child of the outermost grid and the parent of the innermost grid.

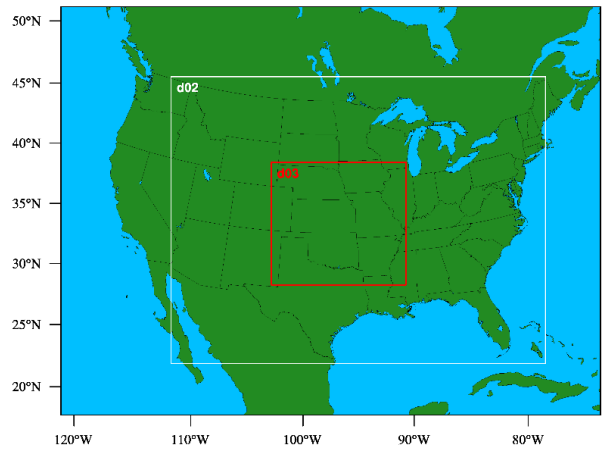

Figure 8. An example of nested limited-area model domains. In this example, the outermost nest (d01) contains 148 x 112 grid points and has a horizontal grid spacing of 36 km. A global or larger-area model provides the lateral boundary conditions for this domain. The intermediate nest (d02) contains 307 x 235 grid points and has a horizontal grid spacing of 12 km. The outermost nest provides the lateral boundary conditions for this nest. The innermost nest (d03) contains 331 x 301 grid points and has a horizontal grid spacing of 4 km. The intermediate nest provides the lateral boundary conditions for this nest.

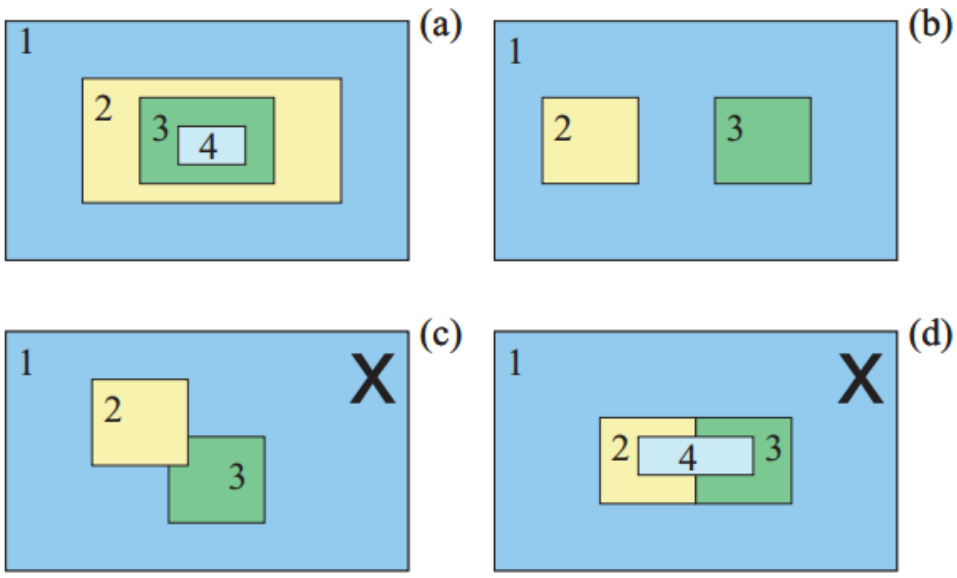

Figure 9. An example of four nested grid configurations, two of which are allowable and two of which are not. In (a), four telescoping domains are depicted. In (b), three domains are depicted, with both domains 2 and 3 having domain 1 as their parent. In (c), three domains are depicted, with domains 2 and 3 overlapping; this is not allowable. In (d), four domains are depicted, with the innermost domain having multiple intermediate domains as its parents; this is also not allowable. Figure obtained from https://opensky.ucar.edu/islandora/object/opensky:2898, their Fig. 7.2.

Nested domain simulations can feature either one-way or two-way feedback. In the case of one-way feedback, the model is first integrated over the outermost domain, the output from which provides initial and lateral boundary conditions to its child domain. The outer domain solution is not affected by the inner domain. In the case of two-way feedback, the model is integrated concurrently for all nested domains. Here, the outer domain(s) also provide initial and lateral boundary conditions to the inner domain(s), but what happens on the inner domain(s) is now able to feed back to the outer domains(s).

Nested domain(s) need not necessarily start and end at the same time as their parent domain(s), nor must they necessarily remain in a fixed location throughout the duration of a numerical simulation. For instance, both research and operational numerical simulations of tropical cyclones will often use a nested domain configuration in which an inner nest moves with the tropical cyclone. Not all models allow such flexibility in nested domain configuration, however.

Furthermore, a nested grid will typically have a horizontal grid spacing that is smaller by a factor of a small odd integer – oftentimes 3:1, but sometimes 5:1 or 7:1 – compared to its parent. As a result, there is an abrupt change in horizontal grid spacing along the lateral boundary between a parent and a child domain. If not treated appropriately, this can compromise forecast quality.

This and other considerations related to lateral boundary conditions will be discussed in a later lecture.

Grid stretching enables the horizontal grid spacing of a limited-area model simulation to steadily decrease from its outermost extent to a specified smaller value in the domain's interior. An example from the Regional version of the Canadian Global Environmental Multiscale (R-GEM) model is given in Fig. 10. As compared to nested grids, there is no abrupt change in horizontal grid spacing between a parent and child domain with grid stretching.

Figure 10. An example of a stretched horizontal grid. In this example, the full limited-area model domain is 353 x 415 grid points, with the centermost 240 x 323 grid points having uniform horizontal resolution. The horizontal grid spacing decreases by 10% per each model grid length as one moves from the periphery of the limited-area domain, where it is identical to that of the global model used to initialize and provide lateral boundary conditions to the simulation (2°), to the center of the limited-area domain, where it is 0.04°. Figure obtained from Yeh et al. (2002, *Mon. Wea. Rev.*), their Fig. 6.